Sustainable Energy, Grids and Networks 21 (2020) 100312

Contents lists available at ScienceDirect

Sustainable Energy, Grids and Networks

journal homepage: www.elsevier.com/locate/segan

One shape parameter-based explicit model for photovoltaic cell and panel

Mostapha Oulcaid [a,*], Hassan El Fadil [a], Leila Ammeh [a], Abdelhafid Yahya [a], Fouad Giri [b]

[a] LGS Lab, ENSA, Ibn Tofail University, 14000, Kénitra, Morocco
[b] Laboratoire d'Automatique de Caen, Université de Caen, Bd Marechal Juin, B.P 8156, 14032, Caen, France

ARTICLE INFO

Article history:
Received 6 July 2019
Received in revised form 2 January 2020
Accepted 11 February 2020
Available online 15 February 2020

Keywords:
Photovoltaic
Explicit model
Cell
Panel
MPPT

ABSTRACT

In this paper, a novel empirical explicit model for photovoltaic (PV) cell and panel is proposed. The model is given by a simple analytic expression and involves only one shape parameter. The model makes it possible to directly calculate the current of the cell/panel corresponding to a given voltage without need for iterative methods or initial conditions. The validation of the proposed model was done through the reproduction of the I–V characteristic and the estimation of the maximum power point (MPP) of several benchmark PV cells and panels of different technologies and under different operating conditions (irradiation and temperature). The good level of similarity between the estimated values using the proposed model and the experimental data demonstrates the validity of the model to simulate the output characteristics and to approximate the MPP easily with good accuracy. Moreover, the model has been compared with several models in the literature which are based on two shape parameters or more. The proposed model shows comparable results to these models even if it is based on fewer parameters.

1. Introduction

Solar energy is available, inexhaustible and clean energy. The efficiency of solar generators increases and the cost of the production decreases continuously. These advantages, among others, make solar energy, especially photovoltaic (PV), a promising alternative solution to polluting sources. One the other hand, the fields of use are more and more varied; from everyday gadgets to giant solar farms. This implies that the conditions under which these PV systems operate (especially irradiation and temperature) are too different and various. Therefore, efficient management of their output power is important. One of the basic aspects of this management is the possibility of modeling and simulating the behavior of photovoltaic cells and panels, and consequently, predicting and improving their production. As a result, a reliable and simple mathematical model has a great advantage as it allows the simulation of the I–V and P-V characteristics of PV generators quickly, easily and with good accuracy.

For this purpose, several models for PV cells and modules have been proposed. The most known one is the model based on one or two diodes [1,2]. This model is widely used and shows good results in terms of accuracy and stability. However, the implicit form of the model makes it difficult to obtain the output current (or power) corresponding to a given voltage. It is therefore necessary to put the model in an explicit form or/and to use numerical algorithms and verify if they converge towards the right solution, hence the importance of having an explicit and reliable model.

The Lambert-W function has been proposed as an approach to eliminate implicitly of this model [3,4]. However, the fact that the Lambert-W function is itself implicit implies the need to involve numerical methods that consume time to solve the problem. Thus, a great effort has been made to find explicit models much simpler and effective.

In [5], authors propose an explicit model in the form of a rational function with four parameters; Open-circuit voltage (V_{oc}), short-circuit current (I_{sc}) and two other shape parameters to be calculated using two experimental points. An empirical model based on exponential function is used in [6]. This model also needs two shape parameters to be determined. "Power law" functions have been widely used to model the I–V characteristics [7–10] (see later). In [11], Padé approximants method was adopted to get a second-order equation whose solution is an explicit expression of the current I. Taylor's series expansions are also used to get the linearization of the diode-based model expression to extract an explicit and less complex model [12,13]. Another empirical model derived from the one-diode model and uses manufacturer data is proposed in [14]. The inputs of this model are irradiance and temperature.

* Corresponding author.
E-mail addresses: oulcaid02@gmail.com (M. Oulcaid), elfadilhassan@yahoo.fr (H. El Fadil), ammeh.leila@gmail.com (L. Ammeh), yaabha2@gmail.com (A. Yahya), giri@greyc.ensicaen.fr (F. Giri).

https://doi.org/10.1016/j.segan.2020.100312
2352-4677/

Nomenclature

V_{oc}	Open-circuit voltage (V)
I_{SC}	Short-circuit current (A)
V_{mpp}	Voltage at MPP point (V)
I_{mpp}	Current at MPP point (A)
P_{mpp}	Power at MPP point (W)
I_{exp}	Measured current (A)
I_{cal}	Calculated current (A)
α	Shape parameter of the proposed model (–)
R_s	Series resistor (Ω)
R_{sh}	Shunt resistor (Ω)
I_o	Reverse saturation current (A)
n	Diode ideality factor (–)
V_α, V_a, V_b	Experimental voltage measurements for shape parameters calculation (V)
I_α, I_a, I_b	Experimental current measurements for shape parameters calculation (A)
A, B, C, C_1, C_2, η, ξ, γ, f, θ, m, α, β_o, Cs	Shape parameters of the models used for comparison (–)
N	Number of samples in a test (–)
$V_{oc,STC}$	Open-circuit voltage at standard test conditions (V).
$I_{SC,STC}$	Short-circuit current at standard test conditions (A).
Ns	Number of series connected cells in a PV module (–).
k	Boltzmann constant (J/K).
q	Electronic charge (C).
V_{th}	Thermal voltage (V)
G	Solar irradiance (W/m^2).
G_{STC}	Solar irradiance at standard test conditions (W/m^2).
T	Cell temperature (K).
T_{STC}	Cell temperature at standard test conditions (K).
$\mu_{V_{oc}}$	Thermal coefficient of the open-circuit voltage (V/°C).
$\mu_{I_{SC}}$	Thermal coefficient of the short-circuit current (A/°C).

In general, the previous models as well as other ones proposed in literature are based either on expressions that are not easy to handle or on an important number of parameters, four or more. On the other hand, some models are suitable only for PV cells; their performance degrades when they are used in case of PV panels. Another important point is the sensitivity of the model to PV cell/panel technology and operating conditions, including irradiance and temperature. These are real challenges for most models in literature (see later).

Taking into consideration the previous points, the present work proposes a simple empirical model based on a sine function. The model is explicit and, in addition to V_{oc} and I_{sc}, only one shape parameter needs to be determined to use the it. The shape parameter can be easily calculated using the maximum power point (MPP) or a point of the I–V curve in the vicinity of the MPP. The validity of the model was evaluated through the generation of I–V curves of several benchmark PV cells and panels which were compared to the experimental data. The comparison was made for various technologies (GaAs, silicon, monocrystalline, polycrystalline) and under different conditions of irradiance and temperature. The model shows good performances in terms of stability and accuracy comparable to those obtained by some models that use more parameters. Moreover, the model is also used to estimate the maximum power point (MPP) of the considered benchmark PV generators. The results show a good correlation between the estimated values and the experimental data.

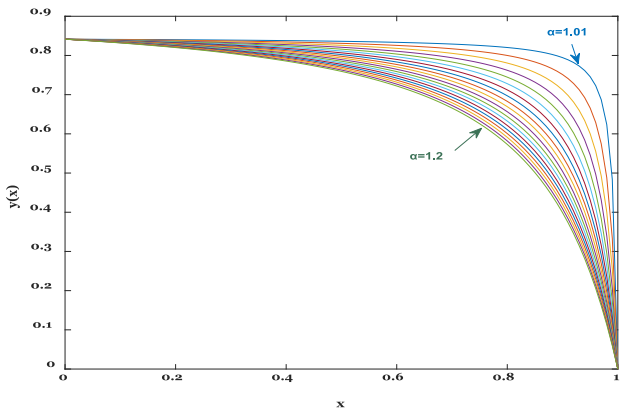

Fig. 1. Plots of the proposed function (Eq. (1)) for increasing values of α: from 1.01 to 1.20 with a step of 0.01.

The rest of the paper is organized as follows: the proposed model is presented and discussed in Section 2. Section 3 deals with the experimental validation of the model and discusses the results of the I–V curves approximation in comparison with some explicit models. The MPP estimation is also investigated in this section. Section 4 concludes the work.

2. Proposed model

The I–V characteristics of photovoltaic cell/module have a remarkable shape. One of the methods for building a simple and reliable model is to look for a mathematical function whose curve is initially close to this shape over a given interval. Then, a set of modifications can be applied to this function so that it describes the behavior of the cell/module with a good precision. The modification is often done via the introduction of certain parameters called "model parameters". The objective is to get a representative model of the cell/module behavior, simple, precise and with minimum of parameters. In this perspective, we have made rigorous studies on several candidate functions. The one adopted in this work is given by:

$$y(x) = sin\left[\frac{\alpha \cdot (x-1)}{x-\alpha}\right], \tag{1}$$

where $\alpha \neq 1$ is a parameter that allows to modify the shape of the curve of the function. Some plots of this function in the interval [0, 1] for different values of the parameter α are given in Fig. 1.

It can be seen from Fig. 1 that the variation of the parameter α makes it possible to modify the shape of the curve in a manner that resembles the variation of the I–V characteristic of a photovoltaic cell/module. This supports the choice of this function.

The expression in Eq. (1) was slightly modified so that it could be used as a valid model. The final model proposed after modification is as follows:

$$I(v) = I_{sc} \cdot sin\left[\frac{\pi}{2} \cdot \frac{\alpha \cdot (V-V_{oc})}{V-\alpha \cdot V_{oc}}\right], \tag{2}$$

with I and V being the current and voltage of the cell/module, respectively. I_{sc} is the short-circuit current. V_{oc} is the open-circuit voltage. α is the shape parameter to be adjusted.

It is clear that the proposed model is explicit and simple. Moreover, if I_{sc} and V_{oc} are available, only the parameter α needs to be determined in order to use the model.

It is easy to verify that: $I(0) = I_{sc} \cdot sin\left[\frac{\pi}{2}\right] = I_{sc}$ and $I(V_{oc}) = 0$. As a result, the curve passes through the two remarkable points: $(0, I_{sc})$ and $(V_{oc}, 0)$. On the other hand, the shape parameter α can be calculated by considering a point (V_α, I_α) in the curvature area of the I–V characteristic (or the point of the maximum power (V_{mpp}, I_{mpp}) if available).

Since the curve already has the general shape of an I–V characteristic (Fig. 1), the introduction of the parameter α allows the shape of the curve to be adjusted so that it passes through the points of the curvature zone (vicinity of the MPP in the range: $[0.6V_{oc}, 0.9V_{oc}]$). In addition, the curve passes also through the two points $(0, I_{sc})$ and $(V_{oc}, 0)$, this allows to adjust the model to a good fit with the different parts of the real (experimental) curve. See next sections.

To calculate α, we consider an experimental point (V_α, I_α). The expression of α is the solution of the following equation:

$$I_\alpha = I_{sc} \cdot sin\left[\frac{\pi}{2} \cdot \frac{\alpha \cdot (V_\alpha - V_{oc})}{V_\alpha - \alpha \cdot V_{oc}}\right]. \tag{3}$$

A simple manipulation of Eq. (3) gives the general expression of α:

$$\alpha = \frac{2 \cdot arcsin\left(\frac{I_\alpha}{I_{sc}}\right) \cdot V_\alpha}{\pi \cdot V_\alpha - \pi \cdot V_{oc} + 2 \cdot arcsin\left(\frac{I_\alpha}{I_{sc}}\right) \cdot V_{oc}}. \tag{4}$$

After determining the expression of the shape parameter, an important point to be discussed is the dependence of the model and the I–V curve that it allows obtaining on irradiance and temperature.

In fact, to use the model to get the I–V curve, three parameters are needed: V_{oc}, I_{SC} and α. It results that the shape of the I–V curve changes according to the variation of these parameters. This means that, if we want to analyze the dependency of the I–V curve on irradiance G and temperature T, we need to see how V_{oc}, I_{SC} and α depend on G and T?

The main parameter α is a function of V_{oc} and I_{SC} (Eq. (4)). It follows that the dependency of α on irradiance and temperature results directly from the dependency of V_{oc} and I_{SC} on these two parameters.

On the other hand, the values of V_{oc} and I_{SC} can be:

- Measured in real time [15]: in this case, the dependency on irradiance and temperature is implicit as the measured values of V_{oc} and I_{SC} vary according to these parameters.
- Estimated in real time using the instantaneous measurement of temperature and irradiance. V_{oc} and I_{SC} can be then calculated using the instantaneous G, T and some manufacturer parameters (from datasheet). Here is an example of expressions that can be used to calculate V_{oc} and I_{SC}:

• The open-circuit voltage $V_{oc}(G, T)$ [16,17]:

$$V_{oc}(G, T) = V_{oc,STC} + \frac{Ns \cdot k \cdot T \cdot n}{q} ln(G) + \mu_{V_{oc}}(T - T_{STC}), \tag{5}$$

where:
$V_{oc,STC}$(V) is the open-circuit voltage at standard test conditions (STC) in.
Ns is the number of series connected cells in the PV. $k = 1.381 \times 10^{-23}$ J/K is the Boltzmann constant.
n is the diode ideality factor.
$q = -1.602 \times 10^{-19}$ C is the electronic charge.
T is the temperature of the cell (K).
$T_{STC} = 289.15$ K is the temperature of the cell at STC.
G is the solar irradiance (W/m^2).
G_{STC} is the solar irradiance at STC (W/m^2).
$\mu_{V_{oc}}$ is the thermal coefficient of the open-circuit voltage (V/°C).

• The shirt-circuit current $I_{SC}(G, T)$ [16]:

$$I_{SC}(G, T) = \frac{G}{G_{STC}}\left[I_{SC,STC} + \mu_{I_{SC}}(T - T_{STC})\right], \tag{6}$$

where:
$I_{SC,STC}$: is the short-circuit current at STC (A).
T is the temperature of the cell (K).
$T_{STC} = 289.15$ K is the temperature of the cell at STC.
G is the solar irradiance (W/m^2).
G_{STC} is the solar irradiance at STC (W/m^2).
$\mu_{I_{SC}}$ is the thermal coefficient of the short-circuit current (A/°C).

The parameters $\mu_{V_{oc}}$, $\mu_{I_{SC}}$, $V_{oc,STC}$, $I_{SC,STC}$, are available in the datasheet of the manufacturer.

In both cases, V_{oc} and I_{SC} depend directly on temperature T and solar irradiance G.

As a conclusion, the main parameter α and the I–V curve depend on T and G through the implicit dependency of V_{oc} and I_{SC} on these two parameters.

In order to show the effectiveness of the proposed model, several I–V characteristics of different cells/modules were reproduced and compared to experimental measurements. In addition, the model was also used to estimate the maximum power point. The results are given and discussed in the next section.

3. Experimental validation of the proposed model

3.1. Estimation of the I-V characteristic

In the first part of the validation, the proposed model was used to estimate the I–V characteristic of several PV cells and modules of different technologies. As the case of several recent works on solar cell modeling or parameters estimation, the present work is based on experimental data of some benchmark cells and panels available in literature and widely used for comparison purposes [18–24]. The reason is to ensure a reasonable comparison with previous works and also for the reproduction of the results.

The obtained results under different irradiance and temperature conditions are compared to the experimental measurements and also with the results obtained with other explicit models.

3.1.1. Case of solar cells

The test of the proposed model starts from the I–V characteristic of two benchmark cells: RTC France silicon solar cell and PVM 752 GaAs thin film cell [25] (operating under full irradiance and a temperature of 33 °C and 25 °C, respectively).

To determine the shape parameter α of the RTC France silicon solar cell, the following experimental data were considered: $V_{oc} = 0.5728$ V, $I_{sc} = 0.7600$ A and the point $(V_\alpha, I_\alpha) = (0.4500\text{ V}, 0.6911\text{ A})$. Then, Eq. (4) was used to calculate the value of the shape parameter. The result is $\alpha = 1.1141$.

Once the value of α was obtained, the I–V curve of the solar cell was approximated. Table 1 shows the values estimated by the model in comparison to the experimental values [25]. In the same table, the IAE (Individual Absolute Error) of each point is given.

As shown in Table 1, IAE values are very low for most points of the I–V characteristic. This shows the ability of the proposed explicit model to simulate the I–V characteristic of this cell.

A similar approach was applied on the PVM 752 GaAs thin film solar cell. The results obtained in the case of the two cells were

Table 1
Estimated and experimental data with the IAE obtained in case of RTC France silicon solar cell.

N°	Measured voltage [V]	Measured current [A]	Calculated current [A]	IAE [A]
1	−0.2057	0.7640	0.7592	0.0047
2	−0.1291	0.7620	0.7596	0.0023
3	−0.0588	0.7605	0.7599	0.0005
4	0.0057	0.7605	0.7599	0.0005
5	0.0646	0.7600	0.7598	0.0001
6	0.1185	0.7590	0.7593	0.0003
7	0.1678	0.7570	0.7584	0.0014
8	0.2132	0.7570	0.7568	0.0001
9	0.2545	0.7555	0.7545	0.0009
10	0.2924	0.7540	0.7511	0.0028
11	0.3269	0.7505	0.7462	0.0042
12	0.3585	0.7465	0.7395	0.0069
13	0.3873	0.7385	0.7303	0.0081
14	0.4137	0.7280	0.7177	0.0102
15	0.4373	0.7065	0.7010	0.0054
16	0.4590	0.6755	0.6784	0.0029
17	0.4784	0.6320	0.6488	0.0168
18	0.4960	0.5730	0.6097	0.0367
19	0.5119	0.4990	0.5585	0.0595
20	0.5265	0.4130	0.4902	0.0772
21	0.5398	0.3165	0.4003	0.0838
22	0.5521	0.2120	0.2801	0.0681
23	0.5633	0.1035	0.1236	0.0201

compared to experimental data [25] and the results obtained with some explicit models proposed in literature. The models investigated for the comparison are given in Table 2.

The values of V_{oc} and I_{sc} used are the same for all models:

* For RTC France silicon solar cell: $V_{oc} = 0.5700$ V, $I_{sc} = 0.7600$ A.
* For PVM 752 GaAs thin film cell: $V_{oc} = 0.9926$ V, $I_{sc} = 0.0998$ A.

For all models that use the maximum power point, the experimental points considered are:

* $V_{mpp} = 0.4500$ V, $I_{mpp} = 0.69119$ A for RTC France silicon solar cell.
* $V_{mpp} = 0.8053$ V, $I_{mpp} = 0.0937$ A for PVM 752 GaAs thin film cell.

All the other parameters of the models are listed in Table 3.

Note that the parameters of each model were calculated using the method proposed by the authors in the corresponding paper. The other parameters, whose methods of computation are not given (e.g. R_s, R_{sh} and n) are obtained from works dealing with parameters approximation of the two cells (see references).

Table 3
Parameters of the used explicit models.

Model	Parameters	RTC France silicon solar cell	PVM 752 GaAs thin film cell
Proposed model	α	1.11416	1.0718
A	A	0.7500	9.9459
	B	0.5729	3.2680
	C	1.5310	12.5001
B	C_2	0.0500	0.0670
	C_1	0.7600	0.0998
C	ξ	0.8823	1.2254
	η	11.0000	11.0000
D	R_s (Ω)	0.0363[a]	0.5000[b]
	R_{sh} (Ω)	53.7185[a]	100.0000[b]
	n	1.4811[a]	1. 7741[b]
	θ	0.6000	0.6000
	γ	0.9860	0.9005
	m	10.2827	13.6825
E	R_s (Ω)	0.0363[a]	0.5000[b]
	R_{sh} (Ω)	53.7185[a]	100.0000[b]
	n	1.4811[a]	1.7741[b]
	I_o (μA)	0.3230[a]	3.2e−5[b]
	α	0.0140	0.0990
	m	8.2426	10.9877
F	R_s (Ω)	0.0363[a]	0.5000[b]
	R_{sh} (Ω)	53.7185[a]	100.0000[b]
	n	1.4811[a]	1.7741[b]
	β_o	25.5908	21.9382
	a	46.5847	1.2092e+04
	b	b(V)[d]	b(V)[d]
	c	c(V)[d]	c(V)[d]
G	C_s	0.1117[c]	0.1117[c]
	η	2.6238	2.2167

[a][26].
[b][25].
[c][10].
[d]Parameters depending on cell voltage.

Fig. 2 shows the experimental I–V curves of the two cells as well as the curves obtained by all models of Table 2.

In order to numerically evaluate the results, two statistical metrics were calculated. These are MBE and RMSE given by:

$$MBE = \frac{1}{N}\sum_{i=1}^{N}(Ii_{exp} - Ii_{cal}), \tag{7}$$

Table 2
Investigated models for the comparison.

Models		Parameters
A[5]	$I = (V_{oc} - v)/(A + B\cdot v^2 - C\cdot v)$	$A = V_{oc}/I_{sc}$, $B = (K_1 - K_2)/K_3$, $C = (K_1\cdot V_a - K_2\cdot V_b)/K_3$. $K_1 = V_a\cdot I_a(V_{oc} - V_b - A\cdot I_b)$, $K_2 = V_b\cdot I_b(V_{oc} - V_a - A\cdot I_a)$, $K3 = V_a\cdot V_b\cdot I_a - I_b\cdot(V_b - V_a)$
B[6]	$I = I_{sc} - C_1 exp(-V_{oc}/C_2)(exp(v/C_2) - 1)$	$C_2 = (V_{mpp} - V_{oc})/\ln(1 - I_{mpp}/I_{sc})$, $C_1 = I_{sc}/(1 - exp(-V_{oc}/C_2))$
C[7]	$I = I_{sc}\cdot(1 - (v/V_{oc})^{\eta})^{(1/\xi)}$	$(I_{mp}/I_{sc})^{\xi} - \eta/(\eta + \xi) = 0$, $\xi = f/((V_{oc}/V_{mpp})^{\eta} - 1)$,
D[8]	$I = I_{sc} - I_{sc}\cdot(1 - \gamma)\cdot v/V_{oc} - \gamma\cdot I_{sc}\cdot(v/V_{oc})^m$	$\gamma = 1 - V_{oc}/(R_{sh}\cdot I_{sc})$, $\mathrm{m} = V_{oc}/(\mathrm{n}\cdot V_{th}\cdot(1 + \theta\cdot\gamma\cdot I_{sc}\cdot R_s/(\mathrm{n}\cdot V_{th})))$
E[9]	$I = I_{sc}\cdot(1 - (v/V_{oc})^m)/(1 + \alpha\cdot v/V_{oc})$	$\alpha = \left(\frac{V_{oc}}{I_{sc}}\right)\frac{1/R_{sh} + \mathrm{Io}\cdot exp(I_{sc}\cdot R_s/(\mathrm{n}\cdot V_{th}))/(\mathrm{n}\cdot V_{th})}{1 + R_s/R_{sh} + \mathrm{Io}\cdot R_s\cdot exp(I_{sc}\cdot R_s/(\mathrm{n}\cdot V_{th}))/(\mathrm{n}\cdot V_{th})}$ $\mathrm{m} = (1 + \alpha)\left(\frac{V_{oc}}{I_{sc}}\right)\frac{1/R_{sh} + \mathrm{Io}\cdot exp(V_{oc}/(\mathrm{n}\cdot V_{th}))/(\mathrm{n}\cdot V_{th})}{1 + R_s/R_{sh} + \mathrm{Io}\cdot R_s\cdot exp(V_{oc}/(\mathrm{n}\cdot V_{th}))/(n\cdot V_{th})}$
F[11]	$I = (1/2a)(-b - \sqrt{b^2 - 4a\cdot c})$	$a = \beta_0^2\cdot R_s^2\cdot(R_p + R_s)$, $\mathrm{b} = \beta_0\cdot R_s(\beta_0\cdot R_s\cdot \mathrm{v} - 2R_p - 2R_s - \beta_0\cdot R_s\cdot R_p\cdot I_{sc} - \beta_0\cdot R_s\cdot R_p\cdot I_{sc}\cdot exp(\beta_0\cdot(\mathrm{v} - V_{oc})))$ $\mathrm{c} = 2\beta_0\cdot R_s\cdot R_p\cdot I_{sc} - 2\cdot\beta_0\cdot R_s\cdot R_p\cdot I_{sc}\cdot exp(\beta_0(\mathrm{v} - V_{oc})) - 2\beta_0\cdot R_s\cdot \mathrm{v}$
G[10]	$I = \begin{cases} I_{sc} * (1 - (1 - I_{mpp}/I_{sc}) * (v/V_{mpp})^{(I_{mpp}/(I_{sc} - I_{mpp}))} & v < V_{mpp} \\ I_{mpp} * V_{mpp} * (1 - ((v - V_{mpp})/(V_{oc} - V_{mpp}))^{\eta})/v & v \geq V_{mpp} \end{cases}$	$Cs = 0.11175$ $\eta = I_{sc} * (V_{oc}/V_{mpp} - 1)/(Cs * I_{mpp})$

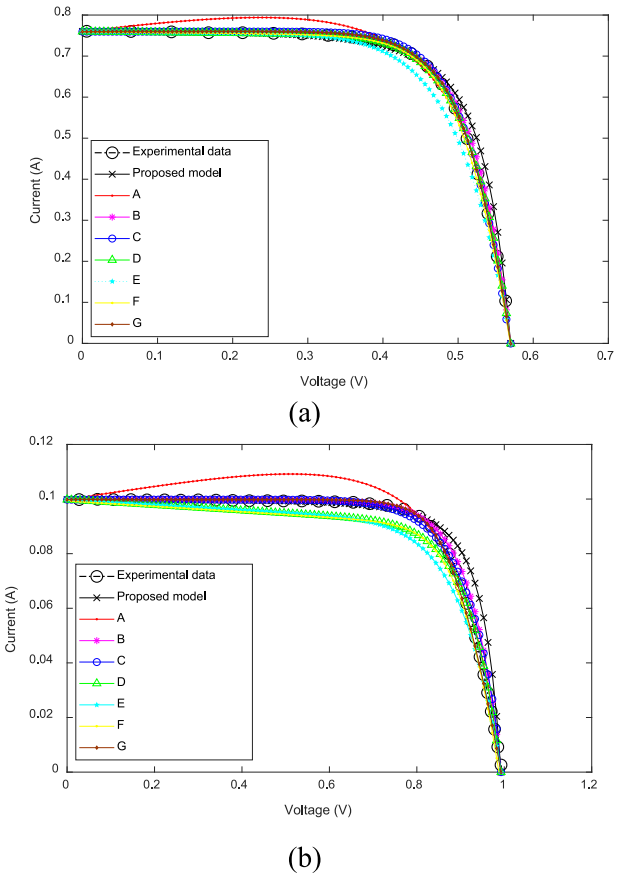

Fig. 2. Obtained I–V characteristics using the proposed model and the models of Table 2 in comparison to experimental curves; (a): RTC France silicon solar cell, (b): PVM 752 GaAs thin film cell.

$$RMSE = \left(\frac{1}{N}\sum_{i=1}^{N}(Ii_{exp} - Ii_{cal})^2\right)^{\frac{1}{2}}, \quad (8)$$

with Ii_{exp} and Ii_{cal} being the experimental and the calculated values of the current, respectively. N is the number of samples. The calculation results are given in Table 4.

According to Fig. 2, it can be noted that, for the two cells considered, the majority of the models showed a good capacity to simulate the real data. In terms of RMSE, the model 'D' has the best result in the case of RTC France silicon solar cell (RMSE = 0.0045086A) while the model 'G' gives the minimal RMSE in the case of the PVM 752 GaAs thin film cell (RMSE = 0.0020253A). A mismatch is observed between the model 'A' and the experimental curve in the low voltage zone. The same can be noted about the models D, E and F in the case of the PVM 752 GaAs thin film cell.

Concerning the proposed model, a slight mismatch can be noticed in the vicinity of V_{oc} in the curve of the second cell. However, a satisfactory similarity is observed between the traced curve and the experimental points of the two cells.

Based on the previous findings, it can be noted that the proposed model gives estimation results of the I–V curves comparable to those obtained by models based on a higher number of parameters and/or iterative calculations.

On the other hand, the fact that the proposed model is based on a minimum of parameters is of great interest; it is easy to switch from one technology to another, from one irradiation/temperature condition to another or even from PV cell to panel by applying a slight modification compared to the other models based on more parameters. This advantage can be clearly noted in the next sub-section dealing with panels.

Table 4
Results of experimental I–V curves estimation using the different models.

Model	RTC France silicon solar cell		PVM 752 GaAs thin film cell	
	MBE [A]	RMSE [A]	MBE [A]	RMSE [A]
Proposed model	−0.0139106	0.0319967	−0.0022908	0.0106891
A	−0.0059597	0.0236090	−0.0022666	0.0055624
B	−0.0054073	0.0111490	−0.0009656	0.0046095
C	−0.0000053	0.0095246	−0.0012317	0.0030074
D	0.0011170	**0.0045086**	0.0025184	0.0041125
E	0.0218919	0.0317432	0.0041842	0.0053994
F	0.0085724	0.0140177	0.0045763	0.0052486
G	0.0006027	0.0076366	0.0011024	**0.0020253**

3.1.2. Case of solar module

To further demonstrate the effectiveness of the proposed model and the possibility to use it for different technologies and different irradiance/temperature conditions with minimal modification, the test applied to the cells was reapplied to different benchmark PV modules. The objective is to simulate the I–V characteristics of these panels and to compare the results to the experimental data.

It is worth noting that the model used in case of PV cells is the same one used for panels; only one shape parameter to adapt.

The panels considered in the case studies are as follows (the experimental I–V curves can be found in the corresponding references):
- STP6-120/36 (polycrystalline, 55 °C) [27].
- STM6-40/36 module (monocrystalline, 51 °C) [27].
- PWP201 (polycrystalline, 45 °C) [28].
- KC200GT (polycrystalline, 25 °C) [29] under different irradiances: 1000 W/m^2, 800 W/m^2, 600 W/m^2, 400 W/m^2 and 200 W/m^2.

In the same way as previously, the characteristics of these panels were simulated using the proposed model in addition to the explicit models of Table 2 and compared to experimental curves. The parameters of each model used in the simulation and their references are listed in Table 5. Experimental and estimated curves are shown in Fig. 3.

With reference to Fig. 3, it can be noted that the behavior of the models vis-à-vis the change of the operating conditions and technologies is very different: The models 'D', 'E' and 'F' have succeeded in reproducing some characteristics (Fig. 3. (c)–(d)) but diverged in the other cases, especially in the case of the STM6-40/36 panel (Fig. 3. (b)). We note also that the efficiency of these models in addition to model 'C' varies strongly with irradiance for the same panel; KC200GT (e.g. Fig. 3. (e)–(h)). On the other side, 'B','G' and the proposed model have performed well; These models show good robustness with respect to the change of technology and operating conditions.

The MBE and RMSE of the considered cases are summarized in Tables 6 and 7, respectively, and graphically represented in Fig. 4.

Based on the results of Tables 6 and 7, one can note that several models show close results with advantage for the model 'B' in terms of RMSE in the case of the panels STM6-40/36 and KC200G (under irradiation of 600 W/m^2 and 400 W/m^2). The model 'G' has the lowest MBE for STM6-40/36 and KC200G (under 1000 W/m^2) panels.

On the other hand, it is clear that the proposed model also has low values of MBE and RMSE in all cases and shows performances comparable with the other models, in particular 'B' and 'G' which give the best results. For example, in the case of the KC200G

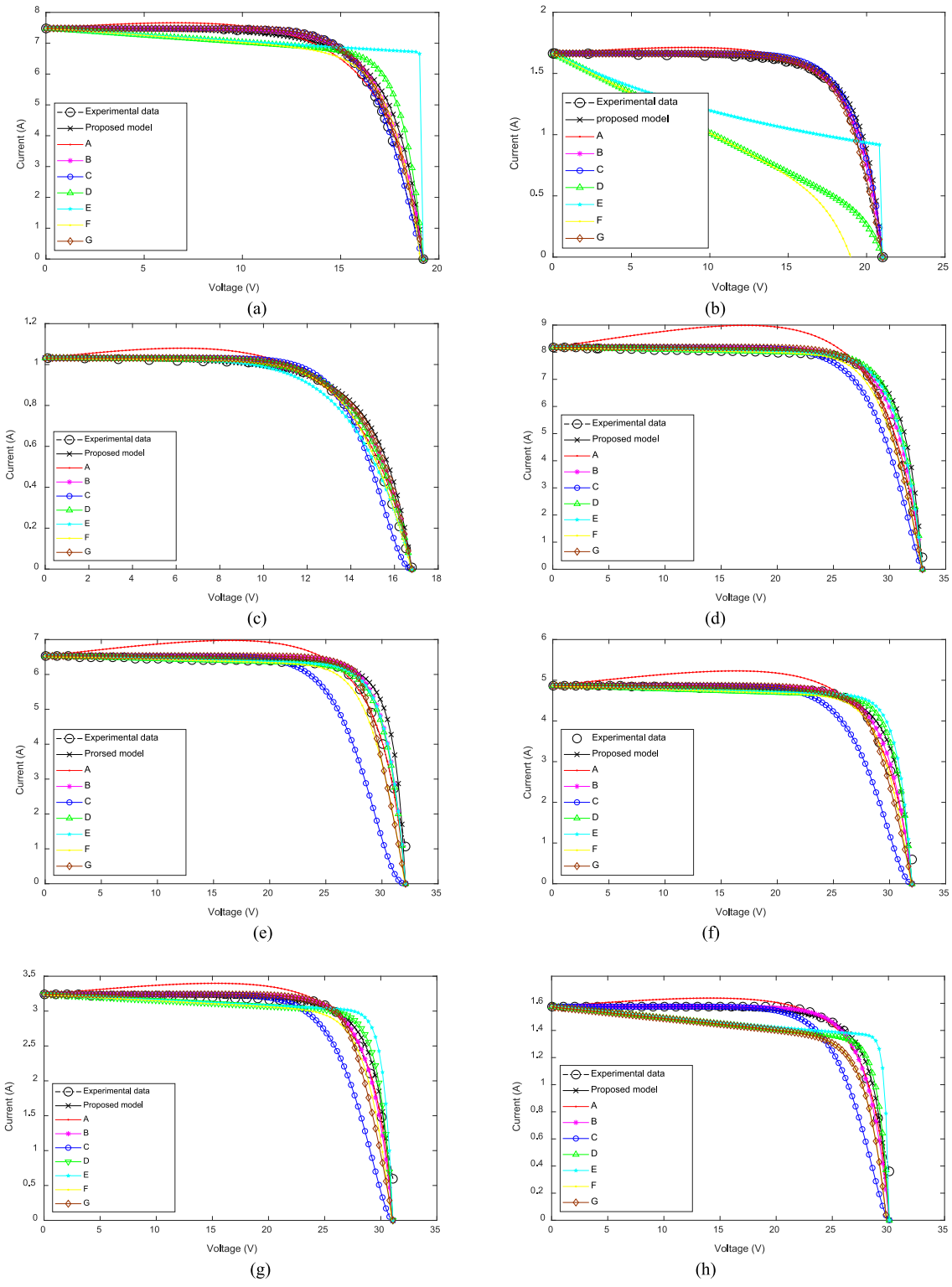

Fig. 3. Estimated I–V characteristics using explicit models in comparison to experimental curves of the different PV panels; (a): STP6-120/36, (b): STM6-40/36, (c): PWP201and KC200GT (d): 1000 W/m^2, (e): 800 W/m^2, (f): 600 W/m^2, (g): 400 W/m^2, (h): 200 W/m^2.

module (under 200 W/m^2), the proposed model has the lowest value in terms of MBE and low RMSE values compared with several models.

Moreover, if we take into consideration that all the models investigated in the comparison are based on a higher number of parameters (4 or more) and some models use parameters that are dependent on voltage and must be recalculated not only for each I–V curve, but for each sample (e.g. the parameters $b(v)$ and $c(v)$ of the model 'F'), one can conclude that the proposed model presents a good compromise between the simplicity and the efficiency of simulating the experimental I–V curve.

Table 8 summarizes the performances of the proposed model in terms of correlation coefficient given by Eq. (9). The coefficient was calculated for all the PV cells and panels considered in this

Table 5
Parameters used for different model to get the I–V characteristic.

Model	Parameters	Photovoltaic panel							
		STP6-120/36	STM6-40/36	PWP201	KC200GT (1000 W/m^2)	KC200GT (800 W/m^2)	KC200GT (600 W/m^2)	KC200GT (400 W/m^2)	KC200GT (200 W/m^2)
Proposed model	α	1.1292	1.1043	1.1650	1.0765	1.0526	1.0750	1.0707	1.0707
A	A	2.5682	12.6398	16.2791	4.0263	4.9157	6.5774	9.5927	19.0910
	B	0.0014	0.0049	0.0184	0.0012	0.0012	0.0017	0.0019	0.0036
	C	0.1490	0.6684	1.1564	0.1538	0.1816	0.2475	0.3527	0.7137
B	C_2	1.7519	1.7394	1.8978	2.2559	1.6724	2.0803	1.9850	1.9407
	C_1	7.4801	1.6630	1.0321	8.1761	6.5300	4.8653	3.2402	1.5754
C	ξ	0.7333	1.1625	0.4387	1.4335	2.5160	2.0550	1.8219	1.6735
	η	11.0000	11.0000	11.0000	11.0000	11.0000	11.0000	11.0000	11.0000
D	R_s (Ω)	0.0046[a]	0.0049[a]	1.2013[a]	0.2574	0.2574	0.2574	0.2574	0.2574
	R_{sh} (Ω)	22.2199[a]	15.4190[a]	981.9823[a]	117.9224	117.9224	117.9224	117.9224	117.9224
	n	1.2601[a]	1.4986[a]	48.6428[a]	1.0170	1.0170	1.0170	1.0170	1.0170
	θ	0.6000	0.6000	0.6000	0.6000	0.6000	0.6000	0.6000	0.6000
	γ	0.8844	0.1802	0.9834	0.9659	0.9583	0.9442	0.9187	0.8381
	m	55.3456	491.8334	8.1352	26.4261	32.3394	43.5024	63.9767	130.7400
E	R_s (Ω)	0.0046[a]	0.0048[a]	1.2013[a]	0.2574[b]	0.2574[b]	0.2574[b]	0.2574[b]	0.2574[b]
	R_{sh} (Ω)	22.2199[a]	15.4190[a]	981.9823[a]	117.9224[b]	117.9224[b]	117.9224[b]	117.9224[b]	117.9224[b]
	n	1.2601[a]	1.4986[a]	48.6428[a]	1.0170[b]	1.0170[b]	1.0170[b]	1.0170[b]	1.0170[b]
	I_o (μA)	2.3350[a]	1.4142[a]	3.4823[a]	5.1200e-4	5.1200e-4	5.1200e-4	5.1200e-4	5.1200e-4
	α	0.1161	0.8200	0.0167	15.6424	19.0975	25.5532	37.2676	2.1529
	m	624.4191	4.7150e+03	6.6357	260.3260	383.8120	678.5195	1.4261e+03	233.8460
F	R_s (Ω)	0.0046[a]	0.0048[a]	1.2013[a]	0.2574[b]	0.2574[b]	0.2574[b]	0.2574[b]	0.2574[b]
	R_{sh} (Ω)	22.2199[a]	15.4190[a]	981.9823[a]	117.9224[b]	117.9224[b]	117.9224[b]	117.9224[b]	117.9224[b]
	n	1.2601[a]	1.4986[a]	48.6428[a]	1.0170[b]	1.0170[b]	1.0170[b]	1.0170[b]	1.0170[b]
	β_o	0.7796	0.6636	0.7499	0.7087	0.7087	0.7087	0.7087	0.7087
	a	2.8454e-04	1.6167e-04	797.7561	3.9329	3.9329	3.9329	3.9329	3.9329
	b	b(V)	b(V)	b(V)	b(V)	b(V)	b(V)	b(V)	b(V)
	c	c(V)	c(V)	c(V)	c(V)	c(V)	c(V)	c(V)	c(V)
G	C_s	0.1117[c]	0.1117[c]	0.1117[c]	0.1117[c]	0.1117[c]	0.1117[c]	0.1117[c]	0.1117[c]
	η	2.8094[c]	2.3605[c]	3.4433[c]	2.0973[c]	1.5819[c]	1.8049[c]	1.8847[c]	1.9526[c]

[a][26].
[b][29].
[c][10].

Table 6
The resulting MBE of real I–V curves estimation using above panel models.

Model	MBE [A]							
	STP6-120/36	STM6-40/36	PWP201	KC200GT (1000 W/m^2)	KC200GT (800 W/m^2)	KC200GT (600 W/m^2)	KC200GT (400 W/m^2)	KC200GT (200 W/m^2)
Proposed model	−0.1393	−0.0054	−0.0349	−0.1552	−0.1324	−0.0359	−0.0127	**0.0115**
A	0.0405	−0.0221	−0.0235	−0.4681	−0.2456	−0.1801	−0.0799	−0.0124
B	−0.1340	−0.0061	−0.0215	−0.1075	−0.1025	−0.0208	**0.0010**	0.0192
C	**−0.0230**	−0.0196	0.0243	−0.1265	−0.1355	−0.0774	−0.0188	0.0133
D	−0.2052	0.6470	−0.0158	−0.0887	**0.0023**	**−0.0041**	0.0370	0.0843
E	−0.4934	0.3740	0.0164	−0.0714	−0.0126	−0.0386	−0.0010	0.0549
F	0.1302	0.7786	**0.0017**	0.1040	1.9679	1.1833	0.6202	0.2487
G	−0.1051	**−0.0029**	−0.0284	**−0.0240**	−0.0026	0.0354	0.0373	0.0366

Table 7
The resulting RMSE of real I–V curves estimation using above panel models.

Model	RMSE [A]							
	STP6-120/36	STM6-40/36	PWP201	KC200GT (1000 W/m^2)	KC200GT (800 W/m^2)	KC200GT (600 W/m^2)	KC200GT (400 W/m^2)	KC200GT (200 W/m^2)
Proposed model	0.3726	0.0220	0.0617	0.3784	0.3708	0.1769	0.1229	0.0696
A	0.1831	0.0335	0.0333	0.6104	0.4066	0.2872	0.1673	0.0762
B	0.2482	**0.0092**	0.0351	0.1880	0.2658	**0.1209**	**0.1155**	0.0687
C	**0.0363**	0.0226	0.0609	0.2628	0.3731	0.2291	0.1211	**0.0659**
D	0.7131	0.7333	0.0248	0.2695	**0.2216**	0.2196	0.1584	0.1263
E	1.1608	0.4221	0.0264	0.2297	0.2383	0.2928	0.2342	0.1594
F	0.4238	0.8679	**0.0049**	0.1942	1.9918	1.2053	0.6241	0.2587
G	0.1595	0.0184	0.0427	**0.1690**	0.2926	0.1757	0.1769	0.0993

work.

$$R^2 = 1 - \frac{\sum_{i=1}^{N}(Ii_{exp} - Ii_{cal})^2}{\sum_{i=1}^{N} Ii_{exp}{}^2}. \quad (9)$$

The values of R^2 obtained in all cases are close to the unity. R^2 = 98.3343% was the lowest value and 99.9792% was the highest one obtained in the case of PVM 752 GaAs thin film cell and STM6-40/36 panel, respectively. These findings show clearly

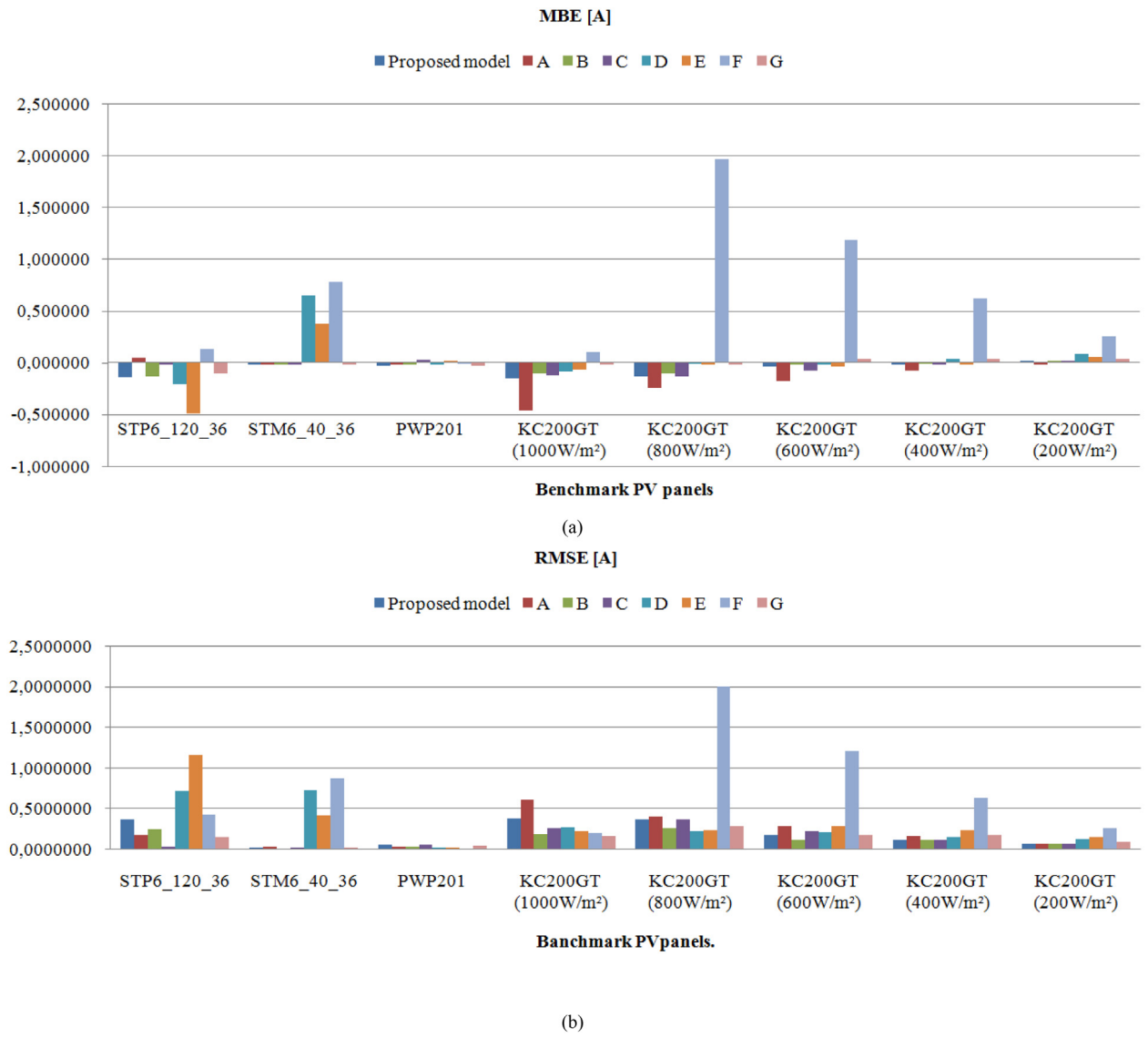

Fig. 4. The errors of experimental I–V curves estimation for all the considered modules; (a) MBE, (b): RMSE.

Table 8
The correlation between experimental and estimated data of the considered cases.

PV cell/panel	R^2 [%]
RTC France silicon	99.7695
PVM 752 GaAs thin film	98.3343
STP6-120/36	99.6578
STM6-40/36	99.9792
PWP201	99.4442
KC200GT (1000 W/m^2)	99.7500
KC200GT (800 W/m^2)	99.6311
KC200GT (600 W/m^2)	99.8488
KC200GT (400 W/m^2)	99.8367
KC200GT (200 W/m^2)	99.7830

that there is a good similarity between the measured I–V curves and the estimated ones using the proposed model.

After demonstrating the ability of the proposed model to simulate the I–V characteristic of PV cells and panels of different technologies and under different climatic conditions, the following section shows the effectiveness of the model in predicting the maximum power point MPP.

3.2. Estimation of the MPP

One of the important parameters to determine for a PV generator is the maximum power point (MPP). A simple model for predicting the MPP quickly and accurately is of great interest. In order to show the effectiveness of the proposed model in achieving this objective, the proposed model was reused to estimate the MPP of all the previous benchmark cells/panels.

The general expression of the output power of a cell/panel using the proposed model is given by:

$$P(V) = V \cdot I(V) = V \cdot I_{sc} \cdot sin\left[\frac{\pi}{2} \cdot \frac{\alpha \cdot (V - V_{oc})}{(V - \alpha \cdot V_{oc})}\right], \tag{10}$$

where V, I and P are the output voltage, current and power, respectively. I_{sc} and V_{oc} are the short-circuit current and the open-circuit voltage, respectively. α is the shape parameter. In all that follows, the values of α for each cell/panel are the same ones obtained and used in the previous section. To find the MPP, it is sufficient to solve Eq. (11) giving the variation of the output power P with respect to the voltage V:

$$\frac{d(P(V))}{dV}_{|V=V_{mpp}} = 0. \tag{11}$$

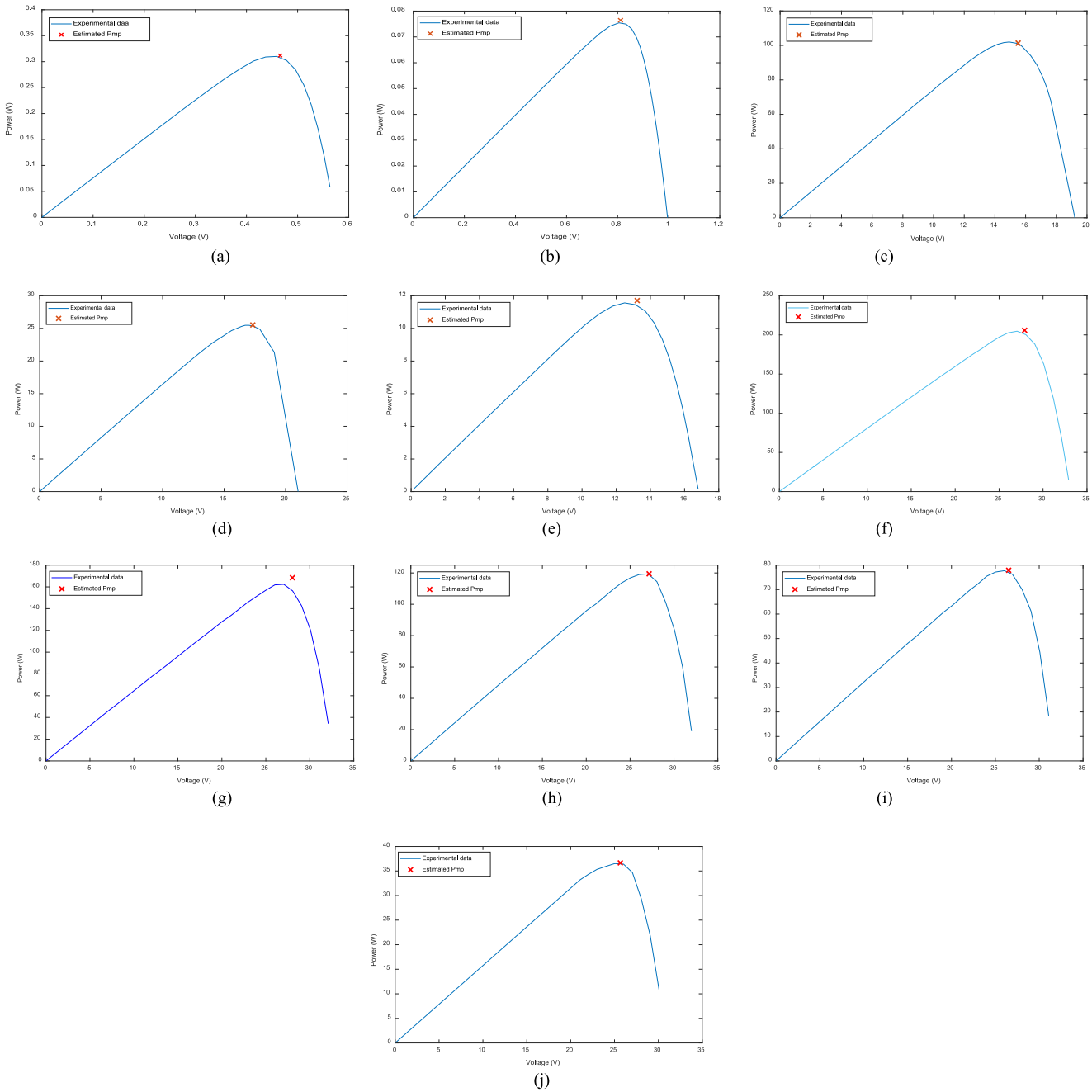

Fig. 5. Estimated MPP and experimental P-V curves of all the considered cases; (a): RTC France silicon solar cell, (b): PVM 752 GaAs thin film cell, (c): STP6-120/36, (d): STM6-40/36, (e): PWP201 and KC200GT (f): 1000 W/m^2, (g): 800 W/m^2, (h): 600 W/m^2, (i): 400 W/m^2, (j): 200 W/m^2.

The solution of this equation is the optimal voltage V_{mp}. Once V_{mp} was obtained, Eq. (10) was used to calculate the corresponding power (MPP). This approach was applied to all the previous cases (cells and panels).

It is worth noting that the estimation of the MPP proposed in this section is useful when the MPP is unknown. In this case, the parameter α can be calculated using any point of the I–V characteristic in the range: $[0.6V_{oc}, 0.9V_{oc}]$.

In Fig. 5, the estimated MPPs using the proposed model are presented with the experimental P-V curves.

On the other hand, Table 9 summarizes the estimated values of V_{mp} and P_{mp} as well as the relative error with respect to the experimental data. The relative error was calculated as follows:

$$Er = \left| \frac{X_{exp} - X_{est}}{X_{exp}} \right| \times 100, \tag{12}$$

X_{exp} Indicates the experimental value and X_{est} is the estimated one.

The results of Fig. 5 show that the estimated MPP is very close to the experimental one, whether in the case of cells or panels. This is numerically supported by the very small values of the relative error given in Table 9, with a maximal error of 3.74% and 0.021% as minimal value. These findings reveal the effectiveness of the proposed model in estimating the MPP with good precision for the different technologies and operating conditions considered in this experimental validation.

Before concluding this section by listing some practical advantages of the proposed model, it would be interesting to discuss the aging aspect that affects the accuracy of the models. In fact, a literature survey shows that aging has a degrading effect on photovoltaic cells and modules which strongly depends on the

Table 9
Results of MPP estimation with relative error.

Solar cell/panel	Experimental V_{mp} [V]	Estimated V_{mp} [V]	Experimental P_{mp} [W]	Estimated P_{mp} [W]	Relative Error in P_{mp} [%]
RTC France silicon	0.459	0.465	0.310	0.311	0.516
PVM 752 GaAs thin film	0.805	0.811	0.075	0.076	1.192
PWP201	12.492	13.226	11.562	11.704	1.233
STM6-40/36	16.980	17.332	25.470	25.526	0.220
STP6-120/36	14.930	15.513	101.971	101.298	0.660
KC200GT (1000 W/m^2)	27.046	27.907	204.737	205.926	0.580
KC200GT (800 W/m^2)	27.046	28.023	162.361	168.427	3.736
KC200GT (600 W/m^2)	27.046	27.172	119.417	119.442	0.021
KC200GT (400 W/m^2)	26.029	26.522	77.722	77.902	0.230
KC200GT (200 W/m^2)	25.022	25.664	36.505	36.651	0.398

design, production process and materials used by the manufacturer. This effect causes losses in the maximum output-power of the cell/module [30] and changes in solar-cell-equivalent-circuit parameters as follows [31]:

- The series resistor R_s and the reverse saturation current I_0 increase;
- The photocurrent I_{ph} and the shunt resistor R_{sh} decrease.

Thus, it is necessary to take this effect into consideration, especially if one uses a model of cell/panel that is based on those parameters.

On the other hand, several studies have been conducted on the behavior of I–V (P-V) curve of photovoltaic generators used for very long time period to evaluate the effect of aging on their output power. Some works on this subject can be consulted in [30–33].

The results of these works show that the aging effect causes an important drop in the output power (current), yet the curve retains its remarkable overall-shape.

Since the model that we propose does not require the knowledge of the parameters (R_s, R_{sh}, n, I_{ph} and I_0) that change under the effect of aging, and given that the basic function (Eq. (1)) used in the model initially has a shape similar to the I–V characteristic which is adjustable by the parameter $\alpha = f(V_{oc}, I_{sc}, V_\alpha, I_\alpha)$ (see Fig. 1), it will be possible, in case of aging, to adjust the shape of the curve obtained by the proposed model using α so that it faithfully represents the new curve of the aged cell/panel. This requires the values of α, V_{oc} and I_{sc} (instantaneously measured or estimated as discussed in Section 2) instead of the five parameters (R_s, R_{sh}, n, I_{ph} and I_0). This is an advantage of the proposed model.

Other practical advantages of the model, especially in improving the overall management of a photovoltaic installation are listed as follows:

– Design of simple, reliable and fast emulators based on the proposed model to simulate the PV installation.

– The proposed model is simple and explicit; it does not require a powerful calculator to use it. This allows more real-time calculation and processing using less powerful and less expensive calculator compared with those used in case of implicit and/or complex models with numerical iterations.

– The ability to identify the MPP easily and to transmit it as a reference to the controller to force the installation to operate at the identified MPP. This has the result of maximizing the output power of the PV installation and increasing the overall gain.

– Thanks to the simplicity of the model, the operator is able to estimate the production of the PV installation easily and at any time. As a result, if a significant difference between the estimated power and the actual one is observed, the operator can deduce that there may be a fault in the installation: DC bus fault, soiling, partial shading, hot spot etc. The operator can then intervene to fix the power-loss problem.

– The proposed explicit model can be used in modeling of complex systems integrating PV arrays such as PV power converters, micro-grids, smart-grids etc.

4. Conclusion

This paper proposes a novel explicit model to simulate the behavior of photovoltaic cells and panels. The advantage of this model is that it is based on a minimum number of parameters; only one shape parameter is needed to be adapted. The model is validated by comparing estimated I–V curves of a variety of benchmark cells and panels to the experimental ones. The comparison is made for different technologies and different scenarios of operating conditions (irradiance and temperature). The model was also compared with several explicit models proposed in literature. The model shows a good compromise between simplicity and precision. This makes the proposed model beneficial in the case of real-time estimation of I–V curves or the MPP prediction easily without using iterative methods or perturbing the system.

Declaration of competing interest

The authors declare that they have no known competing financial interests or personal relationships that could have appeared to influence the work reported in this paper.

CRediT authorship contribution statement

Mostapha Oulcaid: Conceptualization, Methodology, Formal analysis, Software, Validation. **Hassan El Fadil:** Project administration, Supervision, Validation. **Leila Ammeh:** Writing - reviewing & editing. **Abdelhafid Yahya:** Software, Visualization, Investigation. **Fouad Giri:** Supervision.

Acknowledgments

This research did not receive any specific grant from funding agencies in the public, commercial, or not-for-profit sectors.

References

[1] Shongwe Samkeliso, Moin Hanif, Comparative analysis of different single-diode PV modeling methods, IEEE J. Photovolt. 5 (3) (2015) 938–946.
[2] K. Ishaque, Z. Salam, H. Taheri, Simple, fast and accurate two-diode model for photovoltaic modules, Sol. Energy Mater. Sol. Cells 95 (2) (2011) 586–594.
[3] A. Jain, A. Kapoor, Exact analytical solutions of the parameters of real solar cells using Lambert W-function, Sol. Energy Mater. Sol. Cells 81 (2) (2004) 269–277.
[4] A. Dehghanzadeh, G. Farahani, M. Maboodi, A novel approximate explicit double-diode model of solar cells for use in simulation studies, Renew. Energy 103 (2017) 468–477.
[5] M. Akbaba, M.A. Alattawi, A new model for I–V characteristic of solar cell generators and its applications, Sol. Energy Mater. Sol. Cells 37 (1995) 123–132.
[6] A. El-Tayyan, An empirical model for generating the IV characteristics for a photovoltaic system, J. Al-Aqsa Unv. 10 (2006) 214–221.
[7] T.O. Saetre, O.-M. Midtg\a ard, G.H. Yordanov, A new analytical solar cell I–V curve model, Renew. Energy 36 (2011) 2171–2176.

[8] S. Karmalkar, S. Haneefa, A physically based explicit J–V model of a solar cell for simple design calculations, IEEE Electron Device Lett. 29 (2008) 449–451.
[9] A.K. Das, An explicit J–V model of a solar cell using equivalent rational function form for simple estimation of maximum power point voltage, Sol. Energy 98 (2013) 400–403.
[10] S. Pindado, J. Cubas, Simple mathematical approach to solar cell/panel behavior based on datasheet information, Renew. Energy 103 (2017) 729–738.
[11] S. Lun, C. Du, C. Xu, An explicit I—V model of solar cells based on padé approximants, in: 2016 Chinese Control and Decision Conference (CCDC), IEEE, 2016, pp. 6169–6172.
[12] S. Lun, C. Du, T. Guo, S. Wang, J. Sang, J. Li, A new explicit I–V model of a solar cell based on Taylor's series expansion, Sol. Energy 94 (2013) 221–232.
[13] S.X. Lun, C.J. Du, J.S. Sang, T.T. Guo, S. Wang, G.H. Yang, An improved explicit I–V model of a solar cell based on symbolic function and manufacturer's datasheet, Sol. Energy 110 (2014) 603–614.
[14] A. Massi Pavan, S. Vergura, A. Mellit, V. Lughi, Explicit empirical model for photovoltaic devices. Experimental validation, Sol. Energy 155 (2017) 647–653, http://dx.doi.org/10.1016/j.solener.2017.07.002.
[15] Y.P. Huang, A rapid maximum power measurement system for high-concentration photovoltaic modules using the fractional open-circuit voltage technique and controllable electronic load, IEEE J. Photovolt. 4 (6) (2014) 1610–1617.
[16] H. Ibrahim, N. Anani, Variations of PV module parameters with irradiance and temperature, Energy Procedia 134 (2017) 276–285.
[17] G. Kanimozhi, H. Kumar, Modeling of solar cell under different conditions by ant lion optimizer with LambertW function, Appl. Soft Comput. 71 (2018) 141–151.
[18] X. Gao, Y. Cui, J. Hu, N. Tahir, G. Xu, Performance comparison of exponential, Lambert W function and special trans function based single diode solar cell models, Energy Convers. Manage. 171 (2018) 1822–1842.
[19] D.T. Cotfas, A.M. Deaconu, P.A. Cotfas, Application of successive discretization algorithm for determining photovoltaic cells parameters, Energy Convers. Manage. 196 (2019) 545–556.
[20] Y. Chen, Y. Sun, Z. Meng, An improved explicit double-diode model of solar cells: Fitness verification and parameter extraction, Energy Convers. Manage. 169 (2018) 345–358.
[21] M. Merchaoui, A. Sakly, M.F. Mimouni, Particle swarm optimisation with adaptive mutation strategy for photovoltaic solar cell/module parameter extraction, Energy Convers. Manage. 175 (2018) 151–163.
[22] A.M. Beigi, A. Maroosi, Parameter identification for solar cells and module using a hybrid firefly and pattern search algorithms, Sol. Energy 171 (2018) 435–446.
[23] V.J. Chin, Z. Salam, Coyote optimization algorithm for the parameter extraction of photovoltaic cells, Sol. Energy 194 (2019) 656–670.
[24] Y.A. Mahmoud, W. Xiao, H.H. Zeineldin, A parameterization approach for enhancing PV model accuracy, IEEE Trans. Ind. Electron. 60 (12) (2013) 5708–5716.
[25] A.R. Jordehi, Enhanced leader particle swarm optimisation (ELPSO): an efficient algorithm for parameter estimation of photovoltaic (PV) cells and modules, Sol. Energy 159 (2018) 78–87.
[26] X. Gao, Y. Cui, J. Hu, G. Xu, Z. Wang, J. Qu, H. Wang, Parameter extraction of solar cell models using improved shuffled complex evolution algorithm, Energy Convers. Manage. 157 (2018) 460–479.
[27] N.T. Tong, W. Pora, A parameter extraction technique exploiting intrinsic properties of solar cells, Appl. Energy 176 (2016) 104–115.
[28] L. Wu, Z. Chen, C. Long, S. Cheng, P. Lin, Y. Chen, H. Chen, Parameter extraction of photovoltaic models from measured IV characteristics curves using a hybrid trust-region reflective algorithm, Appl. Energy 232 (2018) 36–53.
[29] J. Ma, K.L. Man, T.O. Ting, N. Zhang, S.-U. Guan, P.W. Wong, Approximate single-diode photovoltaic model for efficient IV characteristics estimation, Sci. World J. 2013 (2013).
[30] A. Skoczek, T. Sample, E.D. Dunlop, The results of performance measurements of field-aged crystalline silicon photovoltaic modules, Prog. Photovolt., Res. Appl. 17 (4) (2009) 227–240.
[31] J. Zhu, M. Koehl, S. Hoffmann, K.A. Berger, S. Zamini, I. Bennett …, F. Aleo, Changes of solar cell parameters during damp-heat exposure, Prog. Photovolt., Res. Appl. 24 (10) (2016) 1346–1358.
[32] G.H. Kang, K.S. Kim, C.H. Park, L. Waithiru, G.J. Yu, H.K. Ahn, D.Y. Han, Current–voltage characteristics with degradation of field-aged silicon photovoltaic modules, in: 21st European Photovoltaic Solar Energy Conference, 2006, pp. 4–8.
[33] D. Polverini, M. Field, E. Dunlop, W. Zaaiman, Polycrystalline silicon PV modules performance and degradation over 20 years, Prog. Photovolt., Res. Appl. 21 (5) (2013) 1004–1015.